J Mater Sci: Mater Med (2008) 19:359–367
DOI 10.1007/s10856-007-3186-3

In vitro studies of novel CaO–SiO_2–MgO system composite bioceramics

Siyu Ni · Jiang Chang · Lee Chou

Received: 24 January 2007 / Accepted: 21 May 2007 / Published online: 3 July 2007

Abstract In this study, a series of CaO–SiO_2–MgO composites with different β-$CaSiO_3$ (CS)/Mg_2SiO_4 (M_2S) composite ratios were prepared to produce new bioactive and biodegradable biomaterials for potential bone repair. The mechanical properties of CS–M_2S composites increased steadily with the increase of M_2S ratios in composites. Dissolution tests in Tris–HCl buffer solution showed obvious differences with different CS initial composite ratio in composites. The dissolution rate increased with the increase of CS composite ratio, which suggested that the solubility of composites could be tailored by adjusting the initial CS/M_2S composite ratio. Formation of bone-like apatite on a range of CS–M_2S composites with CS weight percentage ranging from 0 to 100 has been investigated in simulated body fluid (SBF). The presence of bone-like apatite layer on the composite surface after soaking in SBF was demonstrated by X-ray diffraction (XRD), field emission scanning electron microscopy (FESEM). The results showed that the apatite formation ability of the CS–M_2S composite with 70% CS was detected after 10 days immersion. In vitro cell experiments showed that the 50 and 70% CS composites supported greater osteoblast-like cell proliferation as compared with pure M_2S ($p < 0.05$). The results of this study suggested that the CS–M_2S composites with 50 and 70% initial CS composite amount might be more suitable for preparation of bone repair materials.

S. Ni (✉)
Institute of Biological Sciences and Biotechnology,
Donghua University, Shanghai 201620, China
e-mail: synicn@dhu.edu.cn

S. Ni · J. Chang
Biomaterials and Tissue Engineering Research Center,
Shanghai Institute of Ceramics, Chinese Academy of Sciences,
Shanghai 200050, China

L. Chou
Department of Biomaterials, Goldman School of Dental
Medicine, Boston University, Boston, MA 02118, USA

Introduction

For hard tissue repair, the controlled bioactivity and degradation of materials are needed to meet different clinical requirements. However, there are also shortcomings of individual material for its intended medical applications. Since no single existing material possesses all the necessary properties required for an ideal bone graft, then the design of composite materials offers an effective way to allow good control of material properties.

Previous studies have showed that bio-glass and glass-ceramic containing CaO and SiO_2 possessed good bioactivity [1, 2], and this CaO–SiO_2 system has been considered as the basis for many of the third generation tissue regeneration materials presently in development [3]. $CaSiO_3$ (CS) ceramics were also found to induce a very fast apatite formation and a high growth rate of the apatite layer in SBF [4–6]. In vivo experiments showed that the CS coating had good osteoconduction [7]. Although CS ceramics possessed good bioactivity, it showed too fast degradation rate and the mechanical strength was not ideal [8, 9]. Recently, Mg_2SiO_4 (M_2S) ceramic has been reported as a novel bioceramic with higher mechanical properties and good biocompatibility [10], while the degradation rate of M_2S ceramics were extremely low, and the apatite-formation ability was also poor [9]. Previously, Nakajima et al. developed MgO containing CaO–SiO_2 based diopside

($CaMgSi_2O_6$) ceramics to be used as biomaterials, and found that diopside had good bioactive and improved mechanical strength as compared with pure CS ceramics [11, 12]. Recently, Wu et al. has investigated akermanite ($Ca_2MgSi_2O_7$) and bredigite ($Ca_7MgSi_4O_{16}$) single-phase ceramics in the CaO–SiO_2–MgO system, and their studies indicated that akermanite and bredigite ceramics not only possessed improved mechanical strength as compared with pure CS ceramics, but also were degradable and revealed apatite-formation ability in SBF. In addition, the ionic products from akermanite and bredigite could stimulate osteoblast proliferation and differentiation [13, 14]. The above-mentioned results indicated that CaO–SiO_2–MgO systems ceramics might be used as novel bioactive materials for bone regeneration. Therefore, a suitable combination of CS with M_2S to produce new composite ceramics in CaO–SiO_2–MgO system might render greater functionality compared to the CS and M_2S alone.

It is a common notion that the chemical composition is one of the important factors, which may affect the properties of materials. Therefore, in this study, CS–M_2S composite bioceramics with varied ratios were prepared to examine the changes in mechanical properties, in vitro dissolution behavior, apatite-formation ability, and the corresponding osteoblastic cell responses to composites with different CS/M_2S composite ratios, which may provide an insight into the design rule of the new composite ceramics with improved properties for bone regeneration in this CaO–SiO_2–MgO system.

Materials and methods

Preparation of CS–M_2S composites

The starting CS powders were synthesized by a chemical precipitation method as described previously [8]. M_2S were prepared by a sol-gel method using reagent-grade magnesium nitrate hexahydrate ($Mg(NO_3)_2 \cdot 6H_2O$) (Sinopharm, Shanghai, China) and colloidal SiO_2 (Sinopharm, Shanghai, China) as precursors with an initial MgO to SiO_2 molar ratio of 2 [10]. Then, the CS powders were mixed with M_2S by ball milling in ethanol for 24 h. The mixed slurry was dried, crushed and sieved through a 300-mesh screen for future use. By changing the initial CS/M_2S ratio (composition of 70 wt% CS–30% wt% M_2S, 50 wt% CS–50% wt% M_2S and 30 wt% CS–70%wt% M_2S, respectively), CS–M_2S composite powders with different ratios could be obtained.

The resulting composite powders were uniaxially pressed at 10 MPa to form a rectangular compact (45.5 × 8.0 × 3.5 mm) using 6% polyvinyl alcohol (PVA-124) (Sinopharm, Shanghai, China) as binder, then followed by a cold isostatic pressing at 200 MPa. The green samples were subsequently sintered in air at as-determined temperatures (CS/M_2S = 7:3: 1,200 °C, CS/M_2S = 5:5: 1,250 °C, CS/M_2S = 3:7: 1,300 °C) for 5 h with a heating rate of 2 °C/min and then furnace cooled. For cell culture tests, disc-shaped pellets 6-mm in diameter and 1.5-mm in thickness were prepared under the same preparation conditions. For comparative studied, single-phase CS and M_2S discs were also prepared according to the methods used in our previous studies [8, 10]. Before the biological test, all ceramic disks were finely polished with a paste containing fine diamond smaller than 1.5 μm.

Characterization of the composites

The surface characteristics and phase compositions of the sintered samples were characterized by scanning electron microscopy (FESEM; JSE-6700F, JEOL, Japan) and X-ray diffraction (XRD; Geigerflex, Rigaku Co., Japan). The porosity of the samples was measured by the Archimedes principle according to ASTM C-20. The linear shrinkage of samples was calculated from the length of the samples before and after sintering. The 3-point bending strength and Young's modulus were measured with a mechanical testing machine (AG-5kNL, Shimadzu Co, Japan) at a crosshead speed of 0.5 mm/min with span length of 30 mm according to the JIS R1601 standard. In this study, five samples of each group were used to test the average porosity, linear shrinkage, and mechanical strength.

Dissolution studies of the composites

The dissolution behavior of the CS–M_2S composite ceramics were estimated by soaking them in Tris–HCl buffer solution (pH = 7.4) at 37 °C for 3, 7, 14, 21, and 28 days with a surface area-to-volume ratio of 0.1 cm^{-1} [15]. The solution was refreshed everyday. At the selected time points, the samples were removed from the solution, gently rinsed with ethanol, and dried at 60 °C for 24 h, then the final weight of each samples were accurately measured. The weight loss (degradation) was expressed as the percentage of the initial weight. Five samples for each material were tested for each condition. The single-phase M_2S disc served as control.

Soaking in simulated body fluid

The apatite formation behavior of the CS–M_2S composites was evaluated by soaking them in simulated body fluid (SBF). The SBF compositions were prepared following the technique described by Kokubo et al. [16]. The samples

were immersed in SBF for 10 days at 36.5 °C with the ratio of surface area (cm^2) to solution volume (mL) of 0.1 [17]. The soaking experiment was carried out in a shaking bath. After soaking, the samples were removed from the SBF solution, gently rinsed with acetone, and then dried at room temperature before further characterization. Apatite-formation on the composite ceramics was characterized with thin-film XRD. The surface microstructures of the samples after soaking were observed by scanning electron microscopy (FESEM; JSE-6700F, JEOL, Japan).

Cell culture

Osteoblast-like cells were isolated from calvaria of neonatal (less than 2 days old) Sprague–Dawley rats by an enzymatic digestive process as described previously [18, 19]. Briefly, the rat calvaria were washed three times in phosphate-buffered saline (PBS, pH = 7.4) and then minced into fragments of about 1 mm in diameter. After washing the bone fragments three times with PBS, the chips of calvaria were digested for 20 min at 37 °C with 0.25% (w/v) trypsin-EDTA solution (Gibco, USA) to diminish fibroblastic contamination. Then the samples were treated with 1 mg/mL collagenase (Sigma) at 37 °C for 90 min to release osteoblast-like cells from the calvaria. The supernatants were centrifuged at 1,000 rpm for 10 min, and then suspended in the RPMI 1640 (Roswell Park Memorial Institute 1640) medium (Gibco, USA) containing 15% (v/v) heat-inactivated fetal calf serum, 1% glutamine, 50 UI/mL penicillin/streptomycin, and incubated in a 75 cm^2 flask at 37 °C under a humidified atmosphere consisting of 5% CO_2. Culture media were refreshed every 2 days. The cells used in our study were between their second and fourth passages.

Cell morphology

Prior to cell seeding, the ceramic discs were ultrasonically degreased, cleaned in 75% ethanol, and autoclaved for 30 min at 120 °C. About 25 μL of culture medium containing 5×10^3 cells were seeded onto the top of the discs, which were previously placed in 48-well culture plates. The cells were allowed to attach to the substrates for 1 h, then 1 mL of fresh culture medium was added to each well and cells were incubated for 7 days in a humidified atmosphere at 37 °C and 5% CO_2. The cell morphology on different CS–M_2S composite ceramics was observed using scanning electron microscopy (JXA-8100, JEOL, Japan). Specimen/cells constructs were washed with PBS solution twice and fixed in 2.5% glutaraldehyde in 0.1 M sodium-phosphate-buffered solutions for 30 min. The fixed cells were washed three times with PBS solution and then dehydrated in ascending concentrations of ethanol (30, 50, 70, 90, 95, 100% (v/v)) for 10 min each. The specimens were prepared for drying by immersion first in 50% alcohol-HMDS (hexamethyldisilazane) solution (v/v) for 10 min and then in pure HMDS for 10 min. They were air dried in a desiccator overnight [20]. The dried specimens were glued onto copper specimen stubs, and sputter-coated with gold before observation.

Cell proliferation assay

For the examination of cell proliferation, the disc samples (Ø 6×1.5 mm) were washed supersonically in acetone and then sterilized. Cells were seeded onto the discs at a density of 5×10^3 cells/disc, and allowed to adhere for 1 h before the wells were gently flooded with medium (1 mL/well). Cell proliferation was evaluated after incubating for 1, 3, and 7 days. Medium was replaced every other day. After selected culture periods (1, 3, and 7 days), the MTT method was used to assess the cell proliferation levels [21]. MTT (Sigma, USA) (3-[4,5-dimethylthiazol-2-yl]-2,5-diphenyltetrazolium bromide) is a yellow tetrazolium salt, which can be enzymatically converted by a living cell to a purple formazan product. The intensity of the color produced is therefore directly proportional to the number of viable cells in culture, and thus to their proliferation in vitro. The absorbance of the color observed can be measured at 590 nm (A590). In brief, after prescribed time period, substrates were rinsed three times using PBS to remove non-adherent cells. Then, ceramic/cell constructs were placed in culture medium containing MTT and incubated in a humidified atmosphere at 37 °C for 4 h. After removal of the supernatants, the samples were transferred into a new tissue culture plate to avoid lysis of cells not located on the materials, and dimethyl sulfoxide (Sinopharm, Shanghai, China) was added to each well to completely dissolve the purple formazan. The optical density (OD) of each well at 590 nm was determined in a microplater reader (ELX 800, Bio-Tek, USA) with a reference wavelength of 620 nm. The individual M_2S disc served as control. Five specimens for each material were tested for each incubation time and each test was performed in triplicate. Results were reported in OD units.

Inductively coupled plasma atomic emission spectroscopy (ICP-AES) measurement

At each culture time point, the samples were taken out and the calcium (Ca), silicon (Si), and magnesium (Mg) ion concentrations in the culture fluids were measured by inductively coupled plasma atomic emission spectroscopy

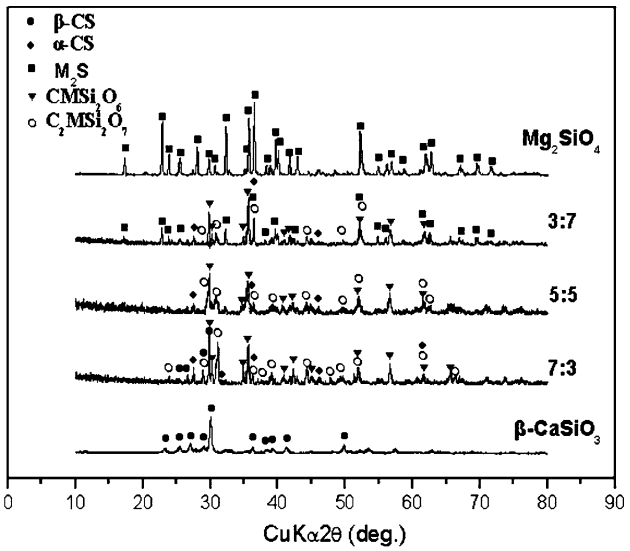

Fig. 1 XRD patterns of CS–M_2S composites with different ratios

(ICP-AES; Varian Co., USA). The samples were diluted 1:10 in distilled water before analysis.

Statistical analysis

Statistical analysis was done using one-way ANOVA with Post Hoc test. All data were collected with $N = 5$ and expressed as means ± standard deviation (SD) in each experiment. Differences were considered statistically significant at $p < 0.05$.

Results

Characterization of samples

The composition of the specimens was analyzed by means of their XRD patterns. With the addition of 30, 50% M_2S (Fig. 1 (7:3, 5:5), respectively), as well as the peaks corresponding to β-CS and α-CS, peaks were also detected for $CaMg(SiO_3)_2$ and $Ca_2MgSi_2O_7$, which originated from the chemical reaction between the CS and M_2S. For the addition of 70% M_2S, XRD analysis (Fig. 1 (3:7)) showed the presence of α-CS, $CaMg(SiO_3)_2$, $Ca_2MgSi_2O_7$, and M_2S, which indicated the CS phase transformed from β- to α-CS completely above 1,200 °C.

The sintering behavior and mechanical properties of specimens sintered at different temperatures are presented in Table 1. It summarizes the values of the porosity, linear shrinkage, bending strength and Young's modulus variations with changes in CS/M_2S initial composite ratio. For single-phase CS ceramic, it has poor sinterability and is difficult to obtain dense sintering body, which displayed a poor mechanical strength. For CS–M_2S composites, the linear shrinkage of the sintered composites was apparently influenced by the initial composite ratio, which displayed a steady increase from 15.9 to 17.3%, and the porosity was 3.5, 1.6, and 2.8%, respectively when the M_2S initial ratio varied from 30 to 70%. In addition, the bending strength of composites was significantly enhanced with the increase of M_2S ratio in composites, and the value reached 168.4 MPa for 70% M_2S composite ratio, but still lower than that of the sintered M_2S (203.4 MPa). However, the Young's modulus of CS–M_2S composites still maintained relative lower value (22.3 GPa) as compared with pure M_2S ceramics (94.9 GPa).

SEM images portray visible differences in the surface microstructure between the as-prepared pure CS, M_2S, and CS–M_2S composites (70, 50, 30% CS respectively) (Fig. 2). It was obvious that the pure CS and M_2S ceramic exhibited a looser and rougher surface with irregular pores than those of CS–M_2S composites and the grain size was about 1–10 μm (Fig. 2a, e). The surface of the CS–M_2S composites (70, 50, 30% CS respectively) became denser with the increase of M_2S composite amount in composites (Figs. 2b, c).

Dissolution studies of the CS–M_2S composites

The dissolution behaviors of the CS–M_2S composites in Tris–HCl solution for time periods ranging from 3 to 28 days are recorded in Fig. 3. It shows that all specimens continue to dissolve after immersion. The resulting weight loss indicated that pure CS ceramics had the highest dissolution rate and solubility compared to other samples over the whole soaking period, reaching up to 27.9% after 28 days. However, the overall amount of M_2S dissolution was minimal and only reached 1.2% at the end of soaking

Table 1 Mechanical properties of the fired bodies sintered at different temperatures for 5 h

Sample	Porosity (%)	Shrinkage (%)	Bending strength σ_f (MPa)	Young's modulus E (GPa)
CS	11.7 ± 0.3	1.6 ± 0.0	35.1 ± 2.0	17.3 ± 1.2
C_7M_3	3.5 ± 0.0	15.9 ± 0.8	112.6 ± 8.4	17.5 ± 2.2
C_5M_5	1.6 ± 0.0	16.1 ± 1.0	122.8 ± 11.7	19.0 ± 7.8
C_3M_7	2.8 ± 0.0	17.3 ± 1.0	168.4 ± 17.0	22.3 ± 7.2
M_2S	6.0 ± 0.1	9.2 ± 0.1	203.4 ± 7.5	94.9 ± 6.3

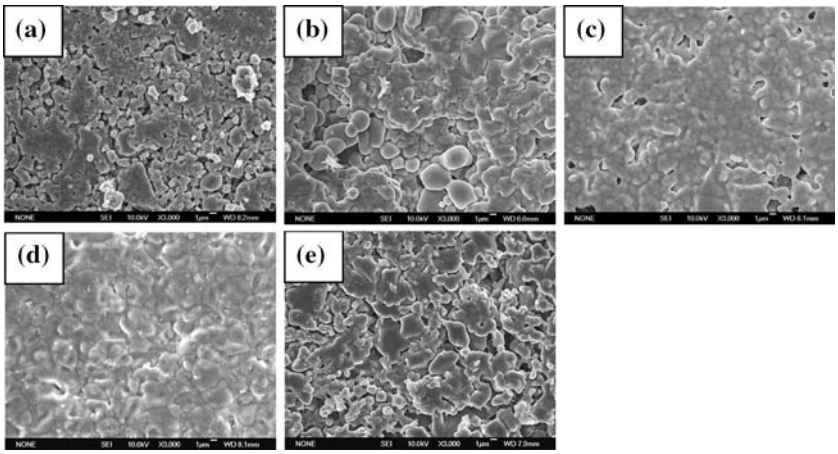

Fig. 2 SEM images of material surfaces before immersion in SBF: (**a**) CS, (**b**) 70% CS + 30% M_2S, (**c**) 50% CS + 50% M_2S, (**d**) 30% CS + 70% M_2S, (**e**) M_2S

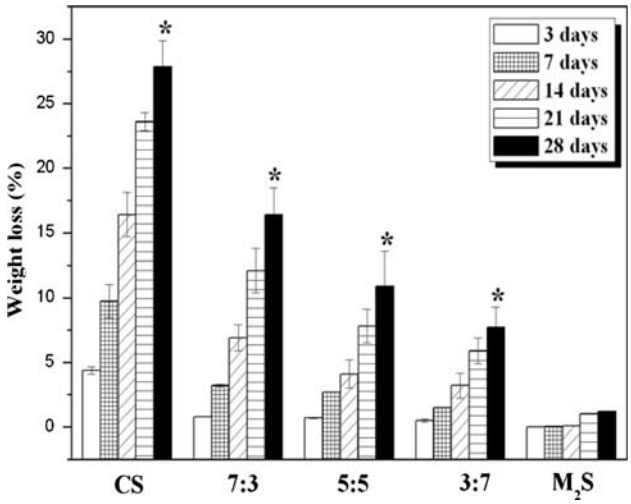

Fig. 3 Weight loss of CS–M_2S composites in Tris–HCl solution for up to 28 days (Data were represented as Mean ± SD, $N = 5$). Note that the composite CS–M_2S dissolved faster than the lower soluble mono-phase M_2S, but slower than the more soluble β-CS. *Significant difference ($p < 0.05$) (compared to the pure M_2S)

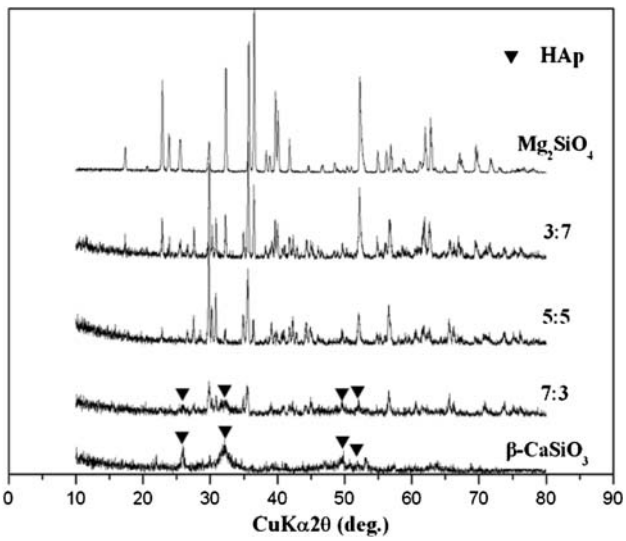

Fig. 4 XRD patterns of CS–M_2S composites with different ratios after immersion in SBF for 10 days

time. As expected, CS–M_2S composites exhibited an intermediate dissolution behavior between those of pure CS and M_2S. Moreover, as the CS composite amount increased, the dissolution rate increased steadily.

Characterization of formed bone-like apatite layer

The XRD patterns of the five specimens after soaking in SBF for 10 days are shown in Fig. 4. The broad additional peaks corresponded to the amorphous apatite granules. After immersion, the apatite phase could be detected for samples with 70 and 100% composite amount of CS. When the CS composite amount decreased to 50%, there were no obvious indications of apatite peaks by X-rays. For pure M_2S ceramic, it was noted that no changes in the diffraction peaks were observed before and after soaking.

The SEM observations of the surfaces for the samples with 70 and 100% CS composite ratio after soaking in SBF for 10 days are showed in Fig. 5. The surfaces of the samples with 70 and 100% CS composite ratio were observed to be covered by a dense apatite layer after immersion for 10 days (Fig. 5a, c). Furthermore, it was evident that some micro-cracks of tortoiseshell like character caused by the shrinkage of the soaked samples in air appeared on the pure CS ceramic, suggesting the formation of a thick apatite layer. A higher magnification examination showed that the surface of the granules was composed of worm-like crystals with typical morphology of hydroxyapatite (HAp) and there are still differences in the particle size between the two samples. For the 100% CS, The size of the crystals was about 100 nm in length and 50 nm in diameter (Fig. 5b). For the 70% CS composite, the particle size was smaller than that of the pure CS ceramic and was about 70 nm (Fig. 5d).

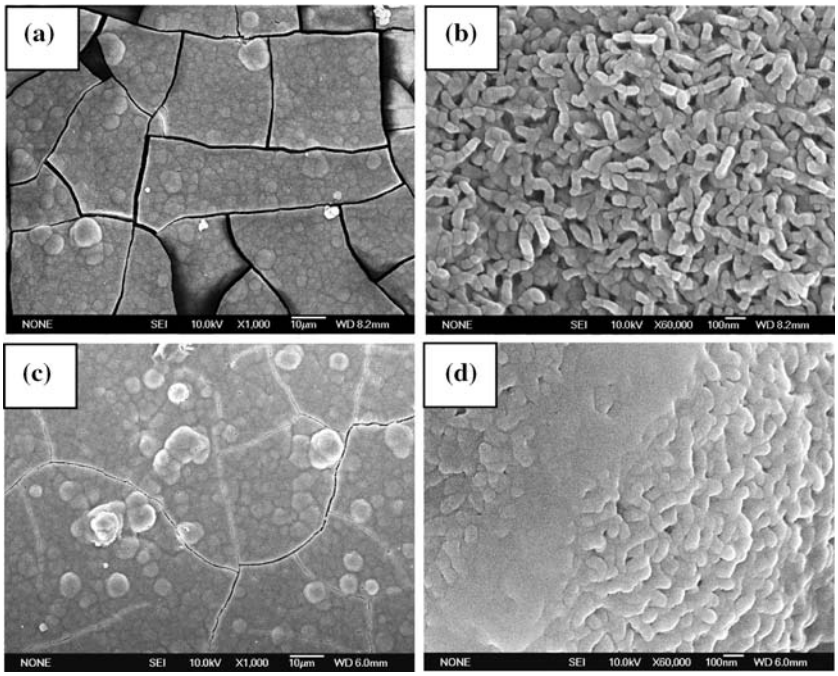

Fig. 5 SEM micrographs of the surfaces of pure CS (**a**, **b**) and CS–M_2S composites (CS/M_2S = 7:3) (**c**, **d**) after immersion in SBF for 10 days

Cell morphology

SEM images of the osteoblast-like cells which were cultured for 7 days on various specimens are presented in Fig. 6. The cells on all specimens were observed to spread well, exhibited intimate contact with the surfaces of the materials. Moreover, the cells formed a flattened sheet and the surface of all the samples were completely covered by the cells and extracellular matrix. However, it seemed to be no significant morphological differences between the various materials containing different composite ratios of CS.

Cell proliferation

Cell proliferation studies were performed at different time points over a period of 7 days (Fig. 7). The OD values provide an indicator of the relative number of cells. The results revealed that there was no significant difference detected among various materials after 1 day of incubation ($p > 0.05$). For all specimens, cells continued to proliferate with the increase of culture time. The changes in cell number on all specimens were quite low in the first 3 days. After culturing for 7 days, the cell numbers increased considerably compared to those at 3 days. Furthermore, for composites with 70 and 50% CS initial composite ratio, the cells proliferated more actively on the composites when compared with the other three samples ($p < 0.05$).

Ionic concentration analysis

After each medium exchange and at the end of the culturing period, the culture fluids were collected to determine

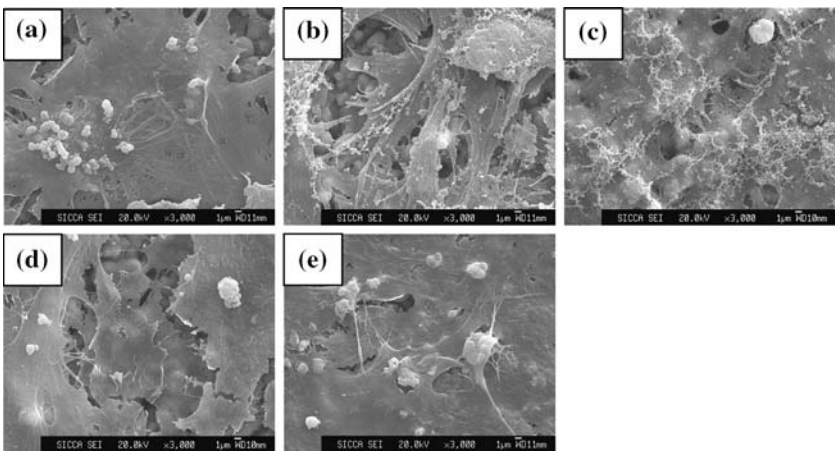

Fig. 6 SEM micrographs of osteoblast-like cells on CS–M_2S composites: (**a**) CS, (**b**) CS/M_2S = 7:3, (**c**) CS/M_2S = 5:5, (**d**) CS/M_2S = 3:7, (**e**) M_2S after 7 days culture

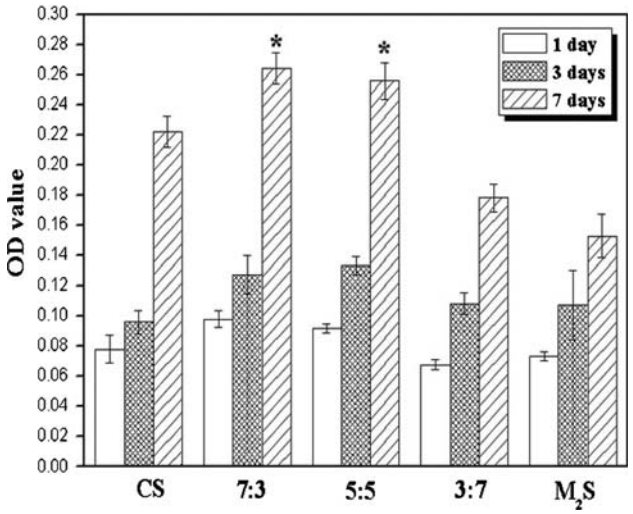

Fig. 7 The cell proliferation on the specimens by MTT assay for 1, 3, and 7 days. Data are presented as the mean ± SD. *Significant difference ($p < 0.05$) (compared to the pure M_2S)

the concentrations of Ca, Si, and Mg ions. The results of the ICP analysis confirmed that all the samples underwent dissolution during the cell culture process (Table 2). Generally, the Ca, Si, and Mg ionic concentrations showed evident differences among the five kinds of materials. The Ca and Si ionic concentrations resulting from pure CS ceramics were much higher, while the Mg ionic concentrations of CS ceramic were lower. In contrast, the Mg and Si ionic concentrations in the presence of pure M_2S ceramic were lowest compared with other samples, which were lightly elevated as compared with those in the pure cell culture medium. In CS–M_2S composites, the Ca, Si, Mg ionic concentration was apparently influenced by the CS/M_2S composite ratio, which displayed a steady decrease with increasing of M_2S composite amount.

Table 2 Ion concentrations released form the different samples into the culture fluid at 1, 3, and 7 days

Samples	Ionic concentration (mmol L^{-1})		
	Ca	Mg	Si
β-CS	3.55[a]	0.40[a]	2.87[a]
	4.24[b]	0.47[b]	3.41[b]
	5.30[c]	0.47[c]	3.42[c]
C_7M_3	2.80[a]	2.57[a]	3.05[a]
	2.94[b]	3.05[b]	3.30[b]
	2.91[c]	3.03[c]	3.07[c]
C_5M_5	2.79[a]	1.76[a]	1.61[a]
	2.91[b]	2.03[b]	1.97[b]
	2.61[c]	1.73[c]	1.53[c]
C_3M_7	2.32[a]	1.10[a]	0.33[a]
	2.25[b]	1.10[b]	0.38[b]
	2.16[c]	1.00[c]	0.31[c]
M_2S	1.34[a]	0.65[a]	0.23[a]
	1.34[b]	0.67[b]	0.26[b]
	1.31[c]	0.66[c]	0.25[c]
Culture medium	1.28	0.47	0

[a] Ion concentrations of culture medium after cultured for 1 day

[b] Ion concentrations of culture medium after cultured for 3 days

[c] Ion concentrations of culture medium after cultured for 7 days

Discussion

The results of this study indicated that the mechanical properties of CS–M_2S composites increased steadily with the increase of initial M_2S composite ratio in composites. Previous studies have shown that the mechanical strengths of the sintered ceramics were correlated with densification [22, 23]. In our study, the CS–M_2S composites showed a markedly improvement on the bending strength values (112.6–168.4 MPa) as compared to the single-phase CS ceramics (35.1 MPa). This can be attributed to the increased densification of sintered composite ceramics. However, the Young's modulus of the CS–M_2S composites displayed a slowly increase from 17.5 GPa to 22.3 GPa and were lower than that of sinter M_2S ceramics (94.9 GPa), but in the range of the published data of cortical bone (7–30 GPa) [2]. Previous studies have indicated that a key requirement for the clinical success of the bioactive ceramics is emphasized to a match of the mechanical behavior of the implant with the tissue to be replaced, and in most cases, the goal is to increase strain to failure and decrease elastic modulus [24, 25]. According to the loading sharing principle of the composite theory, the bioactive ceramics with overhigh elastic modulus are liable to induce bone resorption owing to the stress shielding that surrounds them [26]. So it is expected to fabricate the bioactive ceramics with elastic modulus analogous to that of human bone. Therefore, it seemed that the whole mechanical properties of CS–M_2S composites were better than those of pure CS and M_2S ceramics. In addition, the CS–M_2S composites in this study were prepared under normal sintering conditions and were not fully dense sintered. Thus, it was assumed that better mechanical strengths for the CS–M_2S composites could be obtained with high density and small grain size of the composites by other special sintering methods, such as the hot-pressing technique and the spark plasma sintering process [27–30].

For bone regeneration, it is expected that the degradation rate of a material should match the process of tissue repair or regeneration. Moreover, dissolubility can be considered as one factor of biodegradation [31]. In this study, CS bioceramics showed a significantly higher dissolution rate than the M_2S bioceramics. It was found that

initial CS composite amount had a significant effect on the dissolution rate of the CS–M_2S composites. This is mainly because the solubility product constants (K_{SP}) of CS (2.5×10^{-8}) is much bigger than that of M_2S (2.2×10^{-17}), and the presence of $CaMg(SiO_3)_2$ and $Ca_2MgSi_2O_7$ reported as being biodegradable phase, which suggested that faster dissolution rate of pure CS ceramics and CS–M_2S composites was mainly determined by the chemical composition of the materials under the condition in this study. Therefore, it is possible to control the dissolution rate of the composites by adjusting the CS amount in the composites. However, more in vivo degradation studies need to be conducted to confirm the changes in degradation properties of the CS–M_2S composites.

The capacity of biomaterials to form bone-like apatite could reflect their potential for bonding with bone. The formation of the bone-like apatite SBF has proven to be useful in predicting the bone-bonding ability of material in vitro. The results in this study revealed that the increase of the composite ratio of M_2S in composites decrease the apatite-formation ability in SBF. The different behavior of materials in SBF could be due to difference in chemical composition of different samples. In the present study, chemical reaction occurred between CS and M_2S and produced new phase $CaMg(SiO_3)_2$ and $Ca_2MgSi_2O_7$. Previous studies has reported that $CaMg(SiO_3)_2$ and $Ca_2MgSi_2O_7$ could induce apatite formation in SBF, but the rate of apatite formation for them (after 7 days) was slower than for CS (within 1 day). Furthermore, M_2S was not able to form apatite layer even after 4 weeks in SBF [9]. These indicated that Mg/Ca ratio had an important effect on the apatite-formation ability in CaO–SiO_2–MgO system ceramics. Vallet-Regí et al. found that increasing Mg content in glass would lead to slow down the rate of formation of the apatite layer. One reason is that the higher Mg–O bond energy decreased the solubility of the glass as compared with the Ca–O bond, thus hindering Ca^{2+} exchanges with H_3O^+ of SBF and subsequent formation of silanol groups. Another reason is that traces of Mg ion reduce the overall rate of seeded calcium phosphate crystallization and markedly delay the transformation of amorphous calcium phosphates to more stable apatite phases [32]. In addition, according to the mechanism of apatite formation on the pure CS surface [33], calcium ions initially release from the sample surface, leaving a hydrated silica layer, which has been reported to provide favorable sites for nucleation and crystallization of the apatite [34]. On the other hand, the dissolution of ions increases the degree of supersaturation of the SBF with respect to apatite, leading to the precipitation of the apatite on the sample surfaces. Furthermore, previous studies have confirmed that the mechanism of the apatite formation of the CaO–SiO_2–MgO system ceramics was similar with that of CaO–SiO_2 based ceramics [13, 14, 35]. Therefore, the dissolution rate of the composites decreased with increasing Mg/Ca ratio of composites in the present study, resulting in the slower Ca ion release and more difficult apatite nucleation, which might be the main factor responsible for the decreased apatite-formation ability.

SEM observations of the cell morphology showed no significant morphological difference among the various materials. However, the variation in the chemical composition of the composites greatly affected the cell proliferation. It was found that the CS–M_2S composite with 50 and 70% CS initial composite ratio supported higher osteoblast-like cells growth compared to the other three samples at 7 days ($p < 0.05$). Recent studies have demonstrated the positive stimulatory effect of extracellular calcium, silicon, magnesium containing ionic products from the dissolution of $CaMg(SiO_3)_2$ and $Ca_2MgSi_2O_7$ at certain concentration range on osteoblast-like cells [13, 14]. In the present study, the ICP results showed that calcium, silicon, and magnesium ions could be released from the CS–M_2S composites into the cell culture media over the course of incubation. However, ionic concentration and different ion combinations that would yield optimum cellular responses is still unclear. At least by the proper degree of calcium, silicon, and magnesium ion released from the composites with 50 and 70% CS initial composite ratio, the cellular responses were considered to be affected significantly. In addition, recent studies showed formation of a surface bone-like apatite layer to be a useful but not the critical stage of reaction for bone regeneration. The key factor for bioactive materials used for either tissue replacement or for tissue regeneration must possess controlled chemical release kinetics that synchronize with the sequence of cellular changes occurring in wound repair. If dissolution rates are too rapid the ionic concentration are too high to be effective. If the rates are too slow the concentrations are too low stimulate cellular proliferation and differentiation [3]. In our study, ionic concentrations of different samples showed obvious differences during cell culture, indicating that it is possible to modulate the release rates of active ions by adjusting the initial composite ratio of CS and M_2S. In conclusion, our results in this study provide valuable information for designing CaO–SiO_2–MgO system composite bioceramics for potential bone regeneration applications.

Conclusions

In this study, a series of CS–M_2S composites with different ratios were prepared by sintering the CS–M_2S composite powder compacts at different temperature. The heat treatment induced a reaction between the CS and M_2S. The

composites obtained were a mixture of CS, M_2S, $CaMg(SiO_3)_2$, and $Ca_2MgSi_2O_7$. Mechanical properties of CS–M_2S composites increased steadily with the increase of M_2S initial composite ratios in the composites. The dissolution rate of the CS–M_2S composites was strongly dependent on the Mg/Ca ratio and CS–M_2S composites with higher initial CS composite amount showed higher dissolution rate. The ability to form bone-like apatite on them was investigated by soaking them in SBF for 10 days, and the results showed that CS–M_2S composites with 70% CS could induce apatite formation. Furthermore, in vitro cell culture experiments indicated that the 50 and 70% CS samples supported higher osteoblast-like cells proliferation compared to the other three samples ($p < 0.05$). Our results suggest that the incorporation of CS into M_2S was a useful approach to obtain composites with improved properties, and the composites with 50 and 70% CS initial composite amount might be promising candidates as bone implant materials because of their proper dissolution rates and better bioactivity.

Acknowledgements This work is supported by the National Basic Science Research Program of China (973 Program) (Grant No. 2005CB522700) and Science and Technology Commission of Shanghai Municipality (Grant No. 02JC14009).

References

1. A. MERROLLLI, P. TRANQUILLI LEALI and P. L. GUIDI, *J. Mater. Sci.: Mater. Med.* **11** (2000) 219
2. L. L. HENCH, *J. Am. Ceram. Soc.* **81** (1998) 1705
3. L. L. HENCH, *J. Mater. Sci.: Mater. Med.* **17** (2006) 967
4. P. SIRIPHANNON, S. HAYASHI, A. YASUMORI and K. OKADA, *J. Mater. Res.* **14** (1999) 529
5. Y. IIMORI, Y. KAMESHIMA, A. YASUMORI and K. OKADA, *J. Mater. Sci.: Mater. Med.* **15** (2004) 1247
6. P. SIRIPHANNON, Y. KAMESHIMA, A. YASUMORI, K. OKADA and S. HAYASHI, *J. Biomed. Mater. Res.* **52** (2000) 30
7. W. C. XUE, X. Y. LIU, X. B. ZHENG and C. X. DING, *Biomaterials* **26** (2005) 3455
8. K. L. LIN, W. Y. ZHAI, S. Y. NI, J. CHANG, Y. ZENG and W. J. QIAN, *Ceram. Int.* **31** (2005) 323
9. S. Y. Ni, in "Study on Preparation and Properties of Calcium Silicate and Its Composites" (National Science and Technology Library, Ph. D. Thesis, Beijing, China, 2006) p. 41
10. S. Y. NI, L. CHOU and J. CHANG, *Ceram. Int.* **33** (2007) 83
11. S. NAKAJIMA, Y. KURIHARA, Y. WAKATSUKI and H. NOMA, *Shikwa Gakuho* **89** (1989) 1709
12. T. KOBAYASHI, K. OKADA, T. KURODA and K. SATO, *J. Biomed. Mater. Res.* **37** (1997) 100
13. C. T. WU, J. CHANG, S. Y. NI and J. Y. WANG, *J. Biomed. Mater. Res. A.* **76A** (2006) 73
14. C. T. WU, J. CHANG, J. Y. WANG, S. Y. NI and W. Y. ZHAI, *Biomaterials* **25** (2005) 2925
15. P. DUCHEYNE, S. RADIN and L. KING, *J. Biomed. Mater. Res.* **27** (1993) 24
16. T. KOKUBO, H. KUSHITANI, S. SAKA, T. KITSGI, T. KITSUGI, T. YAMAMURO, *J. Biomed. Mater. Res.* **24** (1990) 721
17. D. C. GREENSPAN, J. P. ZHONG and G. P. LATORRE, *Bioceramics* **7** (1994) 55
18. C. G. BELLOWS, J. E. AUBIN, J. N. M. HEERSCHE and M. E. ANTOSZ, *Calcif. Tissue Int.* **38** (1986) 143
19. S. L. ISHAUG, M. J. YASZEMSKI, R. BIZIOS and A. G. MIKOS, *J. Biomed. Mater. Res.* **28** (1994) 1445
20. Y. JOSSET, F. NASRALLAH, E. JALLOT, M. LORENZATO, O. DUFOUR-MALLET, G. BALOSSIER and D. LAURENT-MAQUIN, *J. Biomed. Mater. Res.* **67** (2003) 1205
21. A. H. CORY, T. C. OWEN, J. A. BARLTROP and J. G. CORY, *Cancer Commun.* **3** (1991) 207
22. J. L. SHI, *J. Mater. Res.* **14** (1999) 1398
23. R. W. RICE, *J. Mater. Sci.* **31** (1996) 1969
24. J. D. CURREY and K. BREAR, *J. Mater. Sci.: Mater. Med.* **1** (1990) 14
25. E. F. MORGAN, N. D. YETKINLER, B. R. CONSTANTZ and R. H. DAUSKARDT, *J. Mater. Sci.: Mater. Med.* **8** (1997) 559
26. D. HULL, T. W. CLYNE, in "An Introduction to Composite Materials", 2nd ed. (Cambridge University Press, Cambridge, 1996) p. 78
27. Z. SHEN, E. ADOLFSSON, M. NYGREN, L. GAO, H. KAWAOKA and K. NIIHARA, *Adv. Mater.* **13** (2001) 214
28. Y. M. KONG, C. J. BAE, S. H. LEE, H. W. KIM and H. E. KIM, *Biomaterials* **26** (2005) 509
29. A. RAPACZ-KMITA, A. ŚLÓSARCZYK and Z. PASZKIEWICZ, *J. Eur. Ceram. Soc.* **26** (2006) 1481
30. L. H. LONG, L. D. CHEN, S. Q. BAI, J. CHANG and K. L. LIN, *J. Eur. Ceram. Soc.* **26** (2006) 1701
31. J. X. LU, M. DESCAMPS and J. DEJOU, *J. Biomed. Mater. Res.* **63** (2002) 408
32. M. VALLET-REGÍ, A. J. SALINAS, J. ROMÁN and M. GIL, *J. Mater. Chem.* **9** (1999) 515
33. X. Y. LIU, C. X. DING and P. K. CHU, *Biomaterials* **25** (2004) 1755
34. P. J. LI, C. OHTSUKI, T. KOKUBO, K. NAKANISHI and N. SOGA, *J. Am. Ceram. Soc.* **75** (1992) 2094
35. N. Y. IWATA, G. H. LEE, Y. TOKUOKA and N. KAWASHIMA, *Colloid Surf. B.* **34** (2004) 239